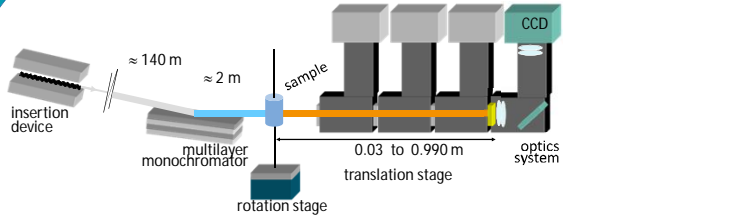


In-line phase contrast tomography

Setup: propagation-based parallel beam phase micro- CT



- X-ray phase contrast imaging offers several advantages versus absorption X-ray imaging
- With coherent X-rays, a simple experimental setup based on **propagation** can be used [1]
- Phase contrast is achieved by moving the detector downstream
- The object is modelled by the **complex refractive index** $n=1-\delta+i\beta$, where δ is the refractive index decrement and β the absorption index
- It depends on the material and the energy of the incoming beam. For soft tissue, at low energies (as used in radiology), δ is three order of magnitude larger than β
- Propagation modelled by **Fresnel diffraction**

- In holotomography [1], images are acquired at:
 - several source-to-sample distances
 - under different angles of rotations
- Phase projections** are obtained by combining these multi-distance projections for each angle θ using phase retrieval.

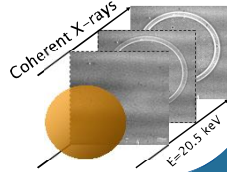


Image reconstruction

- Modeling of the Direct Problem**
 - Attenuation B and phase shift ψ induced by the object described as projections perpendicular to the propagation direction z , with $\mathbf{x}=(x,y)$

$$B(\mathbf{x}) = \frac{2\pi}{\lambda} \int \beta dz \text{ and } \psi(\mathbf{x}) = \frac{2\pi}{\lambda} \int \delta dz$$
 - At each angle θ , the interaction between the object and the X-ray can be described as a transmittance function

$$T_{\theta}(\mathbf{x}) = \exp[-B_{\theta}(\mathbf{x}) + i\psi_{\theta}(\mathbf{x})]$$
 - The free space propagation over a distance D can be modeled by the Fresnel transform involving the propagator P_D

$$T_{\theta,D}(\mathbf{x}) = (T_{\theta} * P_D)(\mathbf{x})$$
 - The intensity recorded by the detector at a distance D is

$$I_{\theta,D}(\mathbf{x}) = |T_{\theta,D}(\mathbf{x})|^2$$
- Inverse problem**
 - Can be split in two steps
 - Phase retrieval:** calculate the phase shift $\psi_{\theta}(\mathbf{x})$ from the phase contrast images at different propagation distances $\{I_{\theta,D}(\mathbf{x}), D=D_1 \dots D_n\}$
 - Ill-posed inverse problem, which requires regularization.
 - $$\hat{\psi}_{\theta}(\mathbf{x}) = \arg \min_{\psi} \sum_D [|T_{\theta,D,\psi}(\mathbf{x}) - I_{\theta,D}(\mathbf{x})|^2 + \alpha | \psi_{\theta}(\mathbf{x}) - \psi_{\theta,0}(\mathbf{x}) |^2]$$
 - Tomographic reconstruction:** reconstruct the 3D refractive index image from the phase shifts $\hat{\psi}_{\theta}(\mathbf{x})$ at different projection angles
 - Usually solved by filtered back-projection.

Regularized phase retrieval

Design of prior

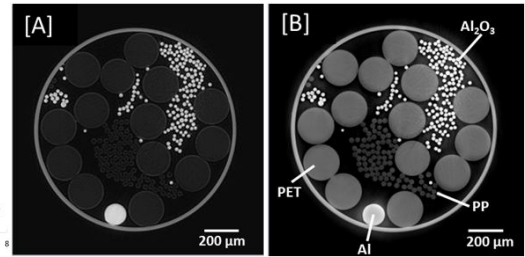
- No prior (i.e. $\psi_{\theta,0}(\mathbf{x})=0$) induces low-frequency noise.
- Possible introduction of **prior** information to alleviate this problem.
- Homogeneous** object: prior is designed assuming that phase is proportional to the attenuation (δ/β -ratio is constant) and applied in the projection domain [3].

$$\psi_{\theta,0}(\mathbf{x}) = f(\mathbf{x}) * \frac{\delta}{2\beta} \ln[I_{\theta,0}(\mathbf{x})]$$

- For **heterogeneous** object of known material, the prior can be designed using several δ/β -ratios:
 - > by thresholding the attenuation scan [4]
 - > by assuming that the δ/β -ratio is a (continuous) function of the attenuation coefficient [5]

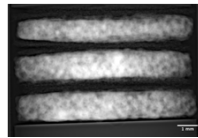
Application on phantom [5]

- Phase retrieval using homogeneous [A] and heterogeneous [B] prior.
- The sample is a phantom composed of multiple wires (Al, PET and PP and Al₂O₃), mounted inside a glass capillary.
- Experimental conditions**
 - 1500 projections
 - 22.5 keV
 - 4 distances
 - Pixel size = 0.7 μm
 - Field of view = 1.4 mm



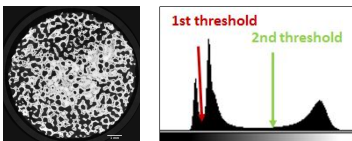
Introduction [6]

- Biomaterial (Skelite®) that can be used for 3D cell culture and artificial bone scaffolds in surgery
- Composed of Si-TCP(67%) and β -TCP/HA (33%)
- 3 scaffolds imaged: discs of 9 mm diameter, seeded with osteoblasts
- Experimental conditions**
 - 2000 projections
 - 30 keV
 - 4 sample-to-detector distances
 - Pixel size=5 μm
 - Field of view = 10.2 mm

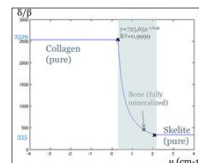


Regularization

- Reconstruction using the **homogeneous approach** (method 1) allows quantification of scaffolds but causes artifacts in soft tissue [7]
- We applied 3 **heterogeneous objects approaches** to improve soft tissue imaging
 - using thresholding (1st and 2nd threshold correspond to methods 2 and 3 respectively)
 - using a functional relationship between the attenuation coefficient and δ/β values (method 4)



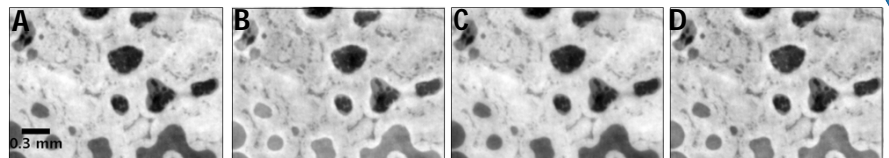
Example of a filtered slice of the attenuation scan, and the corresponding histogram: the histogram is clearly tri-modal, so that 2 different thresholds are possible. They were used in method 2 and method 3.



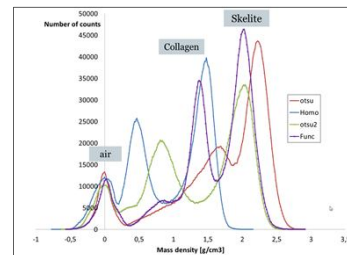
Functional relationship between the attenuation and the δ/β values, used in method 4

Application on 3D cell cultures

Results

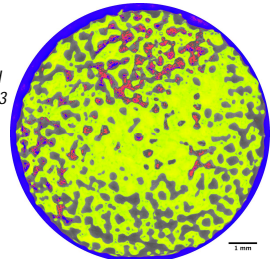


Crop of a reconstructed slice, using homogeneous approach [A], heterogeneous approach with 1st threshold [B] or 2nd threshold [C], and heterogeneous approach with a functional relationship [D].



Histograms of mass densities of the reconstructed slice with the 4 methods

Thresholded slice reconstructed with method 3



- Theoretical mass densities:**
 - $\rho(\text{air})=1.3 \cdot 10^{-3} \text{ g/cm}^3$
 - $\rho(\text{Collagen})=1 \text{ g/cm}^3$
 - $\rho(\text{Skelite}^{\circledR})=1.8 \text{ g/cm}^3$

- Only 3 modes are visible using methods 1 and 2, while we can distinguish 4 modes with methods 3 and 4.
- Method 1 presents fringes around soft tissue
- Phase contrast artefacts are visible using methods 2 and 4.
- Method 3 seems more quantitative, and image quality is improved with regards to the other methods.

Conclusions

- Heterogeneous object approaches can clearly improve image quality
- Choice of good parameters (threshold, function) is of crucial importance

Perspectives

- Introduce spatial constraints in prior, i.e. reconstruction while getting rid of the glass capillary
- Further quantitative studies using a calibrated phantom for example.

Acknowledgements